

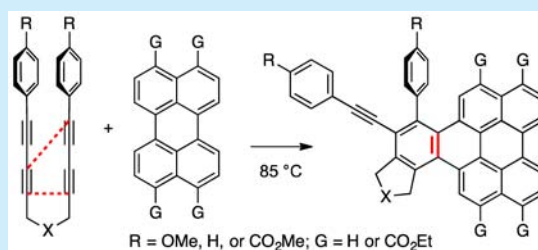
Reactions of HDDA-Derived Benzyne with Perylenes: Rapid Construction of Polycyclic Aromatic Compounds

Feng Xu, Xiao Xiao, and Thomas R. Hoye*

Department of Chemistry, University of Minnesota, Minneapolis, Minnesota 55455, United States

S Supporting Information

ABSTRACT: Benzyne produced by the thermal cycloisomerization of tetrayne substrates [i.e., by the hexadehydro-Diels–Alder (HDDA) reaction] react with perylenes to produce novel naphthoperylene derivatives. Cyclic voltammetry and absorption and emission properties of these compounds are described. DFT studies shed additional light on the dearomatization that accompanies the reaction as well as some of the spectroscopic behavior.

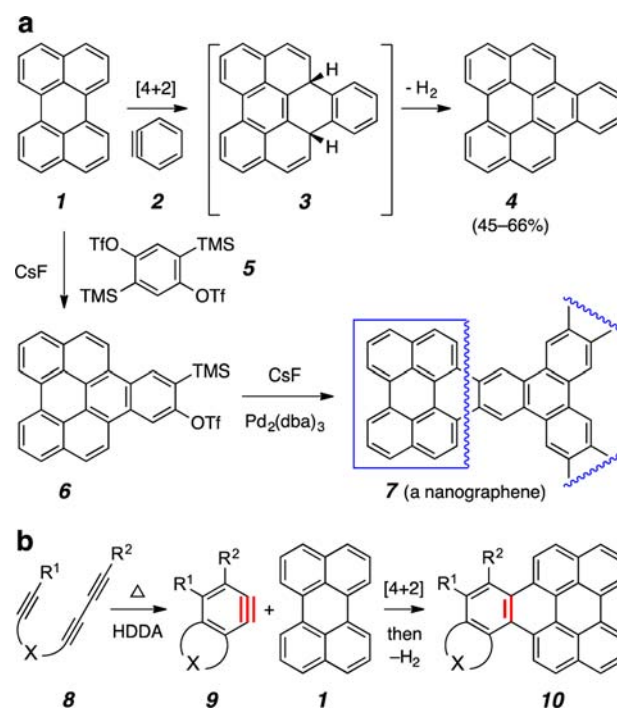


Polycyclic aromatic compounds (PACs) have long been important not only from fundamental theoretical and structural perspectives but also because of their biological and environmental impact, especially with respect to their carcinogenicity.¹ More recently, PACs have attracted considerable attention because of their promising applications in optoelectronic materials such as organic light-emitting diodes, organic field-effect transistors, and organic photovoltaic cells.² The development of facile and efficient strategies for creating novel PACs remains of significance in the fields of both chemistry and materials.³

Strategies for the synthesis of π -extended PACs based on de novo construction of the aromatic cores often leads to lengthy and/or inefficient routes. One way to circumvent this limitation is by starting from a building block that already contains multiple aromatic rings. Perylene (**1**) has been employed in this role to good advantage.⁴ Examples particularly relevant to the work reported here are shown in Scheme 1a. *o*-Benzyne (**2**) adds in [4 + 2] fashion to **1** to give naphtho[1,2,3,4-*ghi*]perylene (**4**) following thermal extrusion of dihydrogen from the intermediate adduct **3**.^{5,6} The bis(benzyne) precursor **5** was recently used to capture **1** under conditions where **6** precipitated from solution, mitigating its further conversion to the second benzyne. Subsequent treatment with fluoride ion, now in the presence of a Pd(0) catalyst, led to the insoluble trimer **7**, which was characterized at atomic resolution by scanning probe microscopy.⁷

The thermal cycloisomerization of a 1,3-diyn bearing a tethered alkyne diynophile (see **8**) leads to the formation of a carbocyclic benzyne moiety (see **9**),⁸ a process we have termed the hexadehydro-Diels–Alder (HDDA) reaction (Scheme 1b).⁹ Recently we have turned our attention to exploring the application of the HDDA reaction to the synthesis of compounds of potential utility in various photonic or electronic materials. One avenue has been to examine the reactions of **9** with **1**. If these were to proceed by

Scheme 1. (a) Synthetic Strategies Based on Perylene for the Synthesis of Some Polycyclic Aromatic Compounds (PACs);^{5b} (b) Possible Routes to PACs through HDDA Cascade Reactions



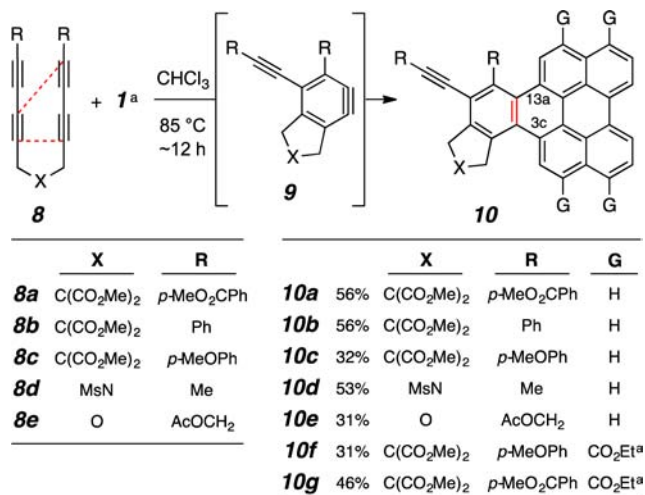
way of the precedent in Scheme 1a, multiple substituents and functionality could readily be incorporated into the naphtho[1,2,3,4-*ghi*]perylene products **10**. We report the results of some of our studies here.

Received: September 23, 2016

Published: October 21, 2016

One of the first reactions we explored was that between perylene (1) and the tetrayne precursor 8a (Scheme 2), which

Scheme 2. Synthesis of Polycyclic Aromatic Compounds 10a–g through Reactions of Tetraynes 8a–e with Perylene (1)



^aIn the reactions leading to 10f and 10g, 1.2 equiv of tetraethyl 3,4,9,10-perylenetetracarboxylate was used in place of 1.

contains a dipropargylated malonate ester linker. This HDDA cascade, effected simply by heating a CHCl₃ solution of 8a and (only) 1.5 equiv of 1 at 85 °C for 10 h, provided an air-stable yellow powder that could be purified by column chromatography to remove excess perylene followed by addition of methanol to a dichloromethane (DCM) solution of this material to precipitate the pure product. Analysis of the 1D and 2D ¹H NMR spectra allowed us to assign the structure as 10a. Resonances corresponding to H⁵, H⁶, and H¹⁰, each of which resides in a bay region of the naphtho[1,2,3,4-*ghi*]perylene moiety, were observed at ca. 8.9 ppm (Figure 1). In contrast, the resonance for H1, the fourth bay region proton, as well as that of H2 resided significantly farther upfield, a reflection of the shielding provided by the adjacent aryl group of the biaryl moiety. No alkyl methine protons were observed, suggesting that two hydrogen atoms had been lost from the presumed initial

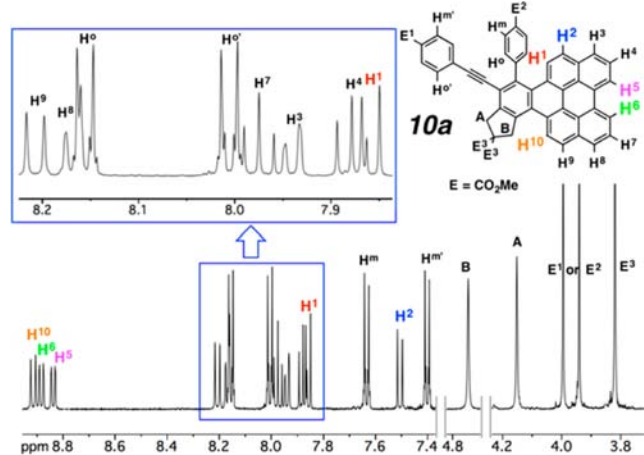


Figure 1. ¹H NMR spectrum of 10a (500 MHz, CDCl₃).

Diels–Alder adduct between 9a and 1 (cf. Scheme 1a) to rearomatize the perylene subunit. The ESI mass spectrum confirmed that fact.

With this result in hand, we explored some aspects of the substrate scope for this reaction (Scheme 2). Tetraynes 8a–c demonstrate that arenes having both electron-poor and -rich character are well-tolerated. The three-atom tether in the tetrayne can include a sulfonamide (8d) or ether (8e) functionality as the central linking group. The electron-deficient perylene derivative containing ester groups at the 3, 4, 9, and 10 positions was also an effective benzyne trapping agent, even when used in a near-stoichiometric quantity (1.2 equiv). It is noteworthy that each of the tetraynes 8a–e can be prepared in just two steps from commercially available alkyne precursors (alkyne bromination and Cadiot–Chodkiewicz cross-coupling; see the Supporting Information (SI)).

In the reaction giving 10g, a small amount (5%) of the bisadducts 11-syn and 11-anti (Figure 2) were also formed.

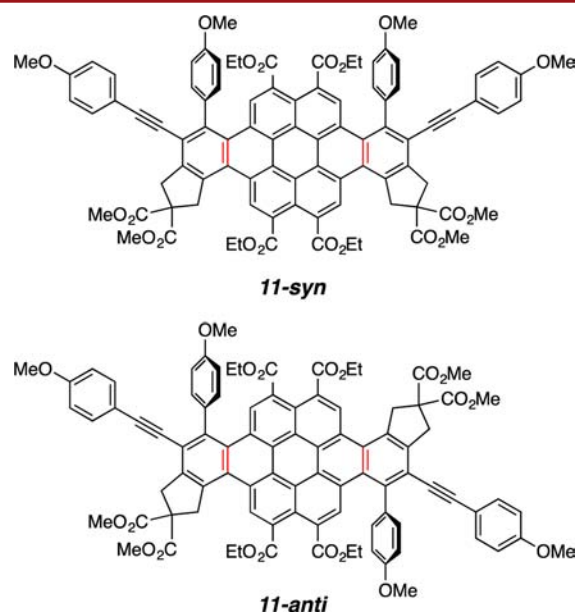


Figure 2. Double adducts from benzyne addition to 10f.

These could be chromatographically separated from 10g but coeluted as a 2:1 mixture that gave an orange powder upon solvent removal. These arise from subsequent head-to-tail and head-to-head additions of the benzyne from 8c to the product 10g, which indicates that dihydrogen was lost during the course of the HDDA cascade reaction. Trace amounts of analogous double adducts were observed in the crude NMR spectra of most of the product mixtures leading to 10a–f, but in those other instances solubility issues made isolation of pure material challenging. Experiments using an excess of tetrayne substrate over the amount of perylene (or perylene tetraester) did not allow the efficient production of any of the expected bisadducts. It is worth noting that perylene has been converted by dienophiles into double-addition adducts in a single operation in only a few instances and never in high yield.¹⁰

DFT [SMD(chloroform)/B3LYP-D3BJ/6-311+G(d,p)//B3LYP/6-31G(d)] calculations were performed on a model system to further probe mechanistic aspects of these reactions. We calculated the energy profile for the reaction between benzyne (2) and perylene (1) (Figure 3). The Diels–Alder

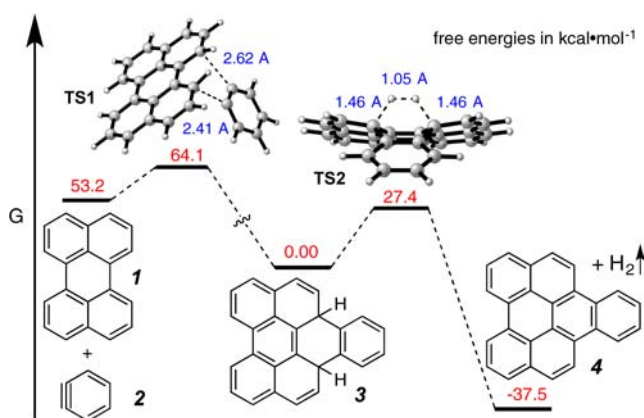


Figure 3. Computed free energy changes for the reaction of benzyne (2) with perylene (1) to give naphthoperylene 4 via extrusion of dihydrogen from the primary Diels–Alder adduct 3.

(DA) reaction is computed to have a free energy of activation (cf. TS1) of ca. 11 kcal·mol^{−1}. That step is highly exergonic because, in addition to the usual driving force for π - to σ -bond change accompanying a DA event, the high degree of strain energy in benzyne more than compensates for the lowering of the perylene aromatic resonance stabilization. We also located a transition structure, TS2 (27.4 kcal·mol^{−1} uphill), that directly connects the DA adduct 3 and product 4. TS2 was computed to have a symmetrical structure, suggesting a concerted loss of dihydrogen. In comparison with the activation energy required for similar concerted dehydrogenation of dihydronaphthalene derivatives (ca. 31 kcal·mol^{−1}, computed)⁶ and dihydrobenzene (42.7 kcal·mol^{−1}, experimental),¹¹ we suggest that the activation energy for the conversion of 3 to 4 would be even lower for the 3c,13a-dihydro adducts leading to products 10 because of the additional π substituents present in 10. In other words, the DA adduct of the HDDA reaction of benzyne and perylene may require an activation energy even less than 27.4 kcal·mol^{−1} for the release of dihydrogen, consistent with the fact that we never detected an intermediate dihydro adduct in any of the reactions reported here.

We measured the cyclic voltammograms (CVs) of dichloromethane (DCM) solutions of all of the adducts 10a–g (see the SI) except for 10d, which showed only limited solubility in all common solvents, including DCM. Two representative CVs (those of 10c and 10g) are shown in Figure 4. The PAC 10c showed a reversible oxidation wave (at 0.69 eV), but no reduction was observed before the onset of solvent

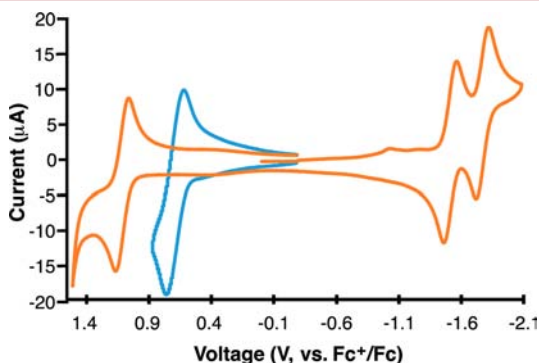


Figure 4. Cyclic voltammograms for 10c (blue) and 10g (orange).

decomposition. All four of the PACs derived from the parent perylene compound (i.e., 10a, 10b, 10c, and 10e) showed very similar behavior ($^{\text{ox}}E_{1/2} = 0.68\text{--}0.71$ eV and no reduction half-wave). The oxidation potentials of the core structures present in this subset of PACs, each an unsubstituted perylene subunit, were insensitive to the electronic character of the remote substituents R present on the phenyl rings.

In contrast, the PAC 10g gave rise to a CV in which both oxidation (1.15 eV) and reduction (−1.50 and −1.75 eV) half-waves were observable. The four carboethoxy groups present on the pyrene-derived core in 10g lowered the reduction potential, a feature that was also seen for 10f (+0.93, −1.68, and −1.92 eV, respectively). In this pair, each having an electron-deficient perylene core, the redox potentials were responsive to the nature of the substituents on the two phenyl rings—OMe for the more easily oxidized and difficult to reduce 10f versus CO₂Me for 10g.

Absorption and fluorescence spectra were also recorded for each of 10a–c and 10e–g (see the SI). Again, representative examples are shown here for 10c and 10g (Figure 5a). The lowest-energy absorption, reflective of the HOMO–LUMO gap, is red-shifted ca. 25 nm in the UV–vis spectrum of the naphthoperylene-tetraester 10g relative to 10c. The emission spectra for both compounds mirror the absorption bands,¹² and again the maximum is red-shifted ca. 25 nm in the spectrum for 10g.

The HOMO and LUMO energies and molecular orbital maps were computed for each of 10a–c and 10e–g [(TD)DFT, B3LYP/6-31G(d)]. In two instances only, the HOMO and LUMO were seen to be located in two significantly different portions of the molecule (Figure 5c). Namely, the HOMO in 10a resided principally on the naphthoperylene core while the LUMO was largely localized on the alkynyl *p*-carbomethoxyphenyl substituents. The reverse was true for 10f, the naphthoperylene-tetraester bearing *p*-methoxyphenyl substituents. It might then be expected that emission from the excited-state singlets for each of these compounds would reflect the intramolecular charge transfer character in each. Indeed (and uniquely among all of the compounds 10), the emission spectra of both 10a and 10f (Figure 5b) are noticeably broader and red-shifted in comparison with those of their counterparts 10b–e (see, e.g., 10c in panel a) and 10g (panel a), respectively. It is notable that the redistribution of orbital density in both of these molecules principally involved the arene substituent on the alkyne (rather than the biaryl) since the former can (and does in the DFT optimization) adopt coplanarity with the naphthoperylene polycycle.

In conclusion, we have described a series of new polycyclic aromatic compounds that can be readily accessed through reaction between HDDA-generated benzyne 9 and perylene (1) or its 3,4,9,10-tetraethyl ester derivative. The reaction is accompanied by in situ aromatization of the initial Diels–Alder adduct, presumably by spontaneous ejection of dihydrogen. Novel bisadducts 11 were observed. CVs showed an interesting lack of sensitivity to electronic substitution for the derivatives of the parent perylene (i.e., 10a–e) but a significant responsiveness to MeO versus MeO₂C substituents in the electron-deficient perylenes 10f versus 10g. Finally, absorption and emission spectra revealed a behavior that was consistent with the differences in the computed HOMO and LUMO maps.

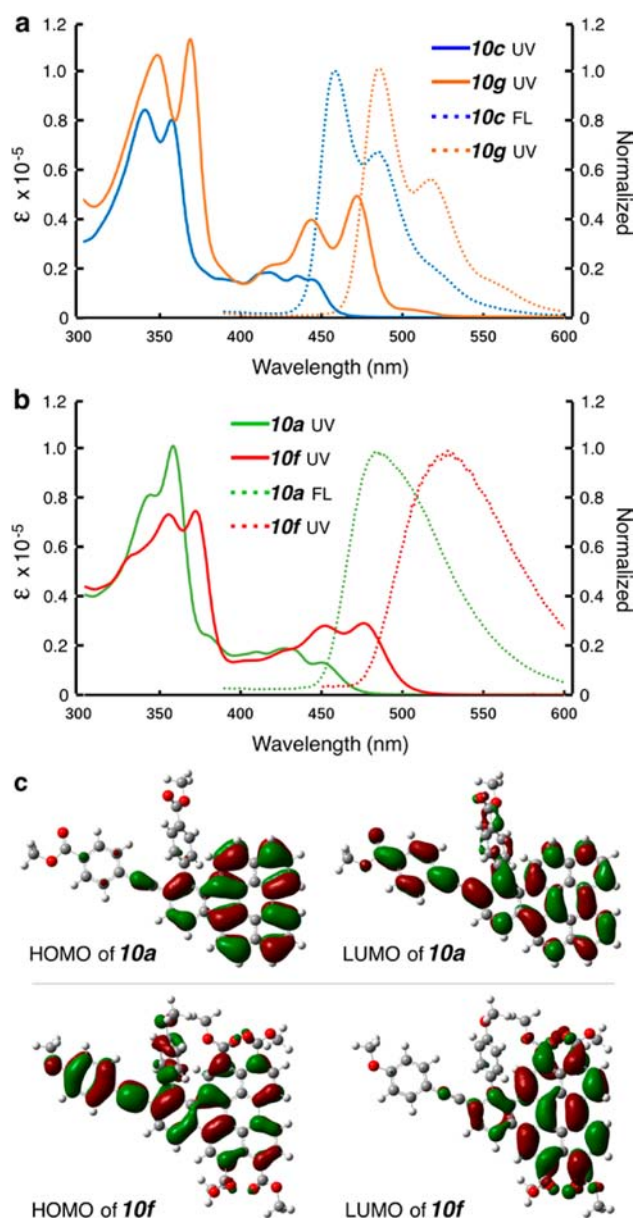


Figure 5. Absorption (unnormalized) and fluorescence (normalized) spectra for (a) 10c (blue) and the tetraester-substituted perylene 10g (orange) and (b) 10a (green) and the electron-deficient perylene 10f (red). (c) DFT-computed HOMOs and LUMOs of 10a and 10f showing the orbital density on the phenyl substituents for the LUMO of 10a and the HOMO of 10f.

■ ASSOCIATED CONTENT

Supporting Information

The Supporting Information is available free of charge on the ACS Publications website at DOI: 10.1021/acs.orglett.6b02878.

Experimental procedures for the synthesis, spectroscopic characterization data, and ^1H and ^{13}C NMR spectra for new compounds; DFT computational methods; and CV and UV and fluorescence spectral data for 10a–c and 10e–g (PDF)

■ AUTHOR INFORMATION

Corresponding Author

*hoye@umn.edu

Notes

The authors declare no competing financial interest.

■ ACKNOWLEDGMENTS

This investigation was supported by a grant awarded by the U.S. Department of Health and Human Services (National Institute of General Medical Sciences, GM65597, and the National Cancer Institute, CA76497). Portions of this work were performed with hardware and software resources available through the University of Minnesota Supercomputing Institute (MSI). Some of the NMR data were recorded using instrumentation purchased with funds awarded through the NIH Shared Instrumentation Grant Program (S10OD011952). We thank Gereon Yee (University of Minnesota) and Joseph J. Dalluge (University of Minnesota) for help in collecting the cyclic voltammetry and HRMS (for 11) data, respectively.

■ REFERENCES

- (1) (a) Harvey, R. G. *Polycyclic Aromatic Hydrocarbons*; Wiley-VCH: New York, 1997. (b) *Polyarenes II*; Siegel, J. S., Wu, Y.-T., Eds.; Topics in Current Chemistry, Vol. 350; Springer: Berlin, 2014.
- (c) *Polyarenes I*; Siegel, J. S., Wu, Y.-T., Eds.; Topics in Current Chemistry, Vol. 349; Springer: Berlin, 2014. (d) Stępień, M.; Gońka, E.; Żyla, M.; Sprutta, N. *Chem. Rev.* **2016**, DOI: 10.1021/acs.chemrev.6b00076.
- (2) *Organic Nanophotonics: Fundamentals and Applications*; Zhao, Y. S., Ed.; Springer: Berlin, 2014.
- (3) Parker, T. C.; Marder, S. R. *Synthetic Methods in Organic Electronic and Photonic Materials: A Practical Guide*; Royal Society of Chemistry: Cambridge, U.K., 2015.
- (4) Markiewicz, J. T.; Wudl, F. *ACS Appl. Mater. Interfaces* **2015**, 7, 28063–28085.
- (5) (a) Stork, G.; Matsuda, K. U.S. Patent 3,364,275, 1968. (b) Fort, E. H.; Scott, L. T. *Tetrahedron Lett.* **2011**, 52, 2051–2053.
- (6) Kocsis, L. S.; Kagalwala, H. N.; Mutto, S.; Godugu, B.; Bernhard, S.; Tantillo, D. J.; Brummond, K. M. *J. Org. Chem.* **2015**, 80, 11686–11698.
- (7) Schuler, B.; Collazos, S.; Gross, L.; Meyer, G.; Pérez, D.; Guitián, E.; Peña, D. *Angew. Chem., Int. Ed.* **2014**, 53, 9004–9006.
- (8) (a) Bradley, A. Z.; Johnson, R. P. *J. Am. Chem. Soc.* **1997**, 119, 9917–9918. (b) Miyawaki, K.; Suzuki, R.; Kawano, T.; Ueda, I. *Tetrahedron Lett.* **1997**, 38, 3943–3946.
- (9) (a) Hoye, T. R.; Baire, B.; Niu, D. W.; Willoughby, P. H.; Woods, B. P. *Nature* **2012**, 490, 208–212. (b) Baire, B.; Niu, D.; Willoughby, P. H.; Woods, B. P.; Hoye, T. R. *Nat. Protoc.* **2013**, 8, 501–508.
- (10) For example, see: Ghosh, A.; Rao, K. V.; George, S. J.; Rao, C. N. R. *Chem. - Eur. J.* **2010**, 16, 2700–2704.
- (11) Ellis, R. J.; Frey, H. M. *J. Chem. Soc. A* **1966**, 553–556.
- (12) Lakowicz, J. R. *Principles of Fluorescence Spectroscopy*; Springer: New York, 2006.